

Laterality effects in functional connectivity of the angular gyrus during rest and episodic retrieval



Buddhika Bellana^{a,b,*}, Zhongxu Liu^{b,d}, John A.E. Anderson^{a,b}, Morris Moscovitch^{a,b}, Cheryl L. Grady^{a,b,c}

^a Department of Psychology, University of Toronto, Canada

^b Rotman Research Institute at Baycrest, Toronto, Canada

^c Department of Psychiatry, University of Toronto, Canada

^d Applied Psychology and Human Development Department, University of Toronto, Canada

ARTICLE INFO

Article history:

Received 7 May 2015

Received in revised form

26 October 2015

Accepted 6 November 2015

Available online 10 November 2015

Keywords:

Angular gyrus

Episodic memory

Default mode network

Retrieval

Rest

Functional connectivity

Recollection network

ABSTRACT

Introduction: The angular gyrus (AG) is consistently reported in neuroimaging studies of episodic memory retrieval and is a fundamental node within the default mode network (DMN). Its specific contribution to episodic memory is debated, with some suggesting it is important for the *subjective* experience of episodic recollection, rather than retrieval of *objective* episodic details. Across studies of episodic retrieval, the left AG is recruited more reliably than the right. We explored functional connectivity of the right and left AG with the DMN during rest and retrieval to assess whether connectivity could provide insight into the nature of this laterality effect.

Methods: Using data from the publically available 1000 Functional Connectome Project, 8 min of resting fMRI data from 180 healthy young adults were analysed. Whole-brain functional connectivity at rest was measured using a seed-based Partial Least Squares (seed-PLS) approach (McIntosh and Lobaugh, 2004) with bilateral AG seeds. A subsequent analysis used 6-min of rest and 6-min of unconstrained, silent retrieval of autobiographical events from a new sample of 20 younger adults. Analysis of this dataset took a more targeted approach to functional connectivity analysis, consisting of univariate pairwise correlations restricted to nodes of the DMN.

Results: The seed-PLS analysis resulted in two Latent Variables that together explained ~86% of the shared cross-block covariance. The first LV revealed a common network consistent with the DMN and engaging the AG bilaterally, whereas the second LV revealed a less robust, yet significant, laterality effect in connectivity – the left AG was more strongly connected to the DMN. Univariate analyses of the second sample again revealed better connectivity between the left AG and the DMN at rest. However, during retrieval the left AG was more strongly connected than the right to non-medial temporal (MTL) nodes of the DMN, and MTL nodes were more strongly connected to the right AG.

Discussion: The multivariate analysis of resting connectivity revealed that the left and right AG show similar connectivity with the DMN. Only after accounting for this commonality were we able to detect a left laterality effect in DMN connectivity. Further probing with univariate connectivity analyses during retrieval demonstrates that the left preference we observe is restricted to the non-MTL regions of the DMN, whereas the right AG shows significantly better connectivity with the MTL. These data suggest bilateral involvement of the AG during retrieval, despite the focus on the left AG in the literature. Furthermore, the results suggest that the contribution of the left AG to retrieval may be separable from that of the MTL, consistent with a role for the left AG in the subjective aspects of recollection in memory, whereas the MTL and the right AG may contribute to objective recollection of specific memory details.

© 2015 Elsevier Ltd. All rights reserved.

1. Introduction

Recruitment of the posterior parietal cortex (PPC), specifically the angular gyrus (AG), has been reported often in the recent episodic memory literature (Benoit and Schacter, 2015; Cabeza et al., 2012; Ciaramelli et al., 2008; Foster et al., 2015; Frithsen and

* Correspondence to: Department of Psychology, University of Toronto, 100 Saint George Street, Toronto, ON, Canada M5S 3G3.

E-mail address: b.bellana@mail.utoronto.ca (B. Bellana).

Miller, 2014; Gilmore et al., 2015; Shimamura, 2014; Skinner and Fernandes, 2007; Spaniol et al., 2009; Vilberg and Rugg, 2008; Rugg and Vilberg, 2013; Wagner et al., 2005). Unlike other core components of traditional episodic memory circuits (e.g., hippocampus, diencephalon, and basal forebrain), where insult typically leads to amnesia (Aggleton, 2012; Aggleton and Brown, 2006; Damasio et al., 1985; Montaldi and Mayes, 2010; Scoville and Milner, 1957), damage to the AG is not associated with such severe memory deficits, though more subtle, restricted deficits are observed (Berryhill, 2012; Schoo et al., 2011; c.f., Ben-Zvi et al., 2015). Stemming from this functional distinction, various neuroanatomical models of episodic memory have been proposed to explain the functional contributions of PPC subregions, including the AG, to episodic memory retrieval (Cabeza et al., 2012; Ciaramelli et al., 2008; Daselaar et al., 2009; Gilmore et al., 2015; Jaeger et al., 2013; Levy, 2012; Nelson et al., 2010; Vilberg and Rugg, 2008; Shimamura, 2011; Simons et al., 2010; Wagner et al., 2005). Though these theoretical models have begun to successfully characterize the nature of AG recruitment during episodic retrieval tasks, they do not account for the laterality differences that are apparent in the literature (Levy, 2012; Seghier, 2013). Studies using functional neuroimaging to explore the neural systems underlying episodic memory reliably report AG recruitment, with a clear bias to the left hemisphere (for meta-analyses, see Humphreys and Lambon Ralph (2014), McDermott et al. (2009) and Spaniol et al. (2009)), regardless of whether verbal or nonverbal stimuli are used (e.g., Spaniol et al., 2009; Vilberg and Rugg, 2007), suggesting that there may be factors contributing to this effect that exist beyond stimulus modality.

To explore the neural basis for the left laterality effect in AG, we examined AG functional connectivity with the default mode network (DMN), a large-scale network associated with the retrieval of episodic memories (Andrews-Hanna et al., 2010, 2014; Daselaar et al., 2009; Huijbers et al., 2012; McCormick et al., 2014; Spreng et al., 2009). The DMN overlaps considerably with regions associated with recollection (Rugg and Vilberg (2013) including autobiographical memory, Maguire (2001), St-Laurent et al. (2011), and recollection-specific regions are thought to be a separable subsystem of the overarching DMN (Andrews-Hanna et al., 2010). Thus, we examined both the similarities and differences in connectivity between the left and right AG during rest and episodic retrieval in two separate experiments. Understanding the differences in connectivity between the left and right AG may provide insight into the left AG laterality effect. If, for example, the left AG shows better connectivity with the DMN during both rest and during retrieval, it would suggest that the reason we see a preference for left AG activity is that it is better integrated into a system that can support episodic memory. Furthermore, by probing intra-DMN connectivity, we can determine which subregions of the DMN support this laterality effect, affording more nuanced inferences regarding the function of both the left and right AG based on the regions with which they are better connected.

We hope to answer three questions: first, do the left and right AG contribute to the DMN to a similar degree during rest? The left preference during memory retrieval may be supported by greater connectivity between the DMN and the left AG at rest, as the laterality effect in activity may emerge because the left AG is simply better integrated, intrinsically, into this memory system. Second, if there are differences in connectivity within the DMN at rest, where do they occur? Relative to the overall network association, this question targets a more nuanced explanation by examining laterality effects within specific subregions of the DMN. Third, how does active retrieval modify the functional connectivity pattern between the bilateral AG and subregions of the DMN? This question allows us to explore directly any

laterality effects in connectivity between rest and active episodic retrieval.

2. Methods

2.1. Overview

We examined the laterality effect in the angular gyrus using functional connectivity analyses in two separate experiments: first, examining connectivity during rest and second, contrasting connectivity during rest and an unconstrained episodic retrieval task. For the first experiment, we used a data-driven multivariate analysis to characterize both similarities and differences in whole-brain connectivity between the left and right angular gyrus. Resting data provides unique insight into differences between the angular gyri in their intrinsic connectivity with the entire brain (Cole et al., 2014), and a useful baseline in comparison to episodic retrieval. Furthermore, the use of a data-driven analysis allowed us to explore the most prominent multivariate patterns of connectivity in our data without any prior definition of network nodes. For the second experiment, we extended the findings of the first experiment with a theoretically driven univariate analysis directly contrasting the left and right angular gyrus connectivity across a set of memory-sensitive DMN nodes, during both rest and episodic retrieval. The inclusion of the retrieval condition in this analysis allowed us to bridge the results between our resting data and the reported laterality effects during active retrieval of episodic memories. Furthermore, since this experiment was restricted to the nodes of the DMN, testing for laterality differences in functional connectivity within these individual nodes was better suited for a contrast-based univariate approach. Different participants were used in each experiment.

2.2. Experiment 1

2.2.1. Participants

Data from 180 younger adults were included in this experiment, acquired from the 1000 Functional Connectome Project (for details, see http://fcon_1000.projects.nitrc.org/). All participants were between 17 and 28 years of age ($M=21.2$, $SD=1.94$) and the sample was collected at the Beijing Normal University. No measure of education was available for this dataset, although a measure of full-scale IQ was available for a subset of 67 participants ($M=125.3$, $SD=8.5$). All participants were healthy, right-handed, and had normal or corrected to normal vision.

2.2.2. Data acquisition and processing

All participants were tested using the Siemens Trio 3-T scanner at the Imaging Center for Brain Research at the Beijing Normal University. A T1-weighted 3D MP-RAGE sequence was used to collect the structural scans ($TR=2530$ ms, $TE=3.39$ ms, flip angle = 7° , $FOV=25.6$ cm², 256×192 matrix, 128 slices of 1.33 mm thickness). In addition, eight-minutes of eyes-closed resting scans were collected from each participant. Resting functional runs were collected with a T2-weighted EPI sequence (240 volumes, $TR=2000$ ms, $TE=30$ ms, flip angle = 90° , $FOV=20$ cm², 64×64 matrix, 30 slices of 5 mm thickness, gap = .6 mm). The raw data were downloaded from the 1000 Functional Connectome Project (http://fcon_1000.projects.nitrc.org/indi/retro/BeijingEnhanced.html), and then preprocessed using the pipeline described below.

The data were preprocessed using the Analysis of Functional Neuroimaging suite (AFNI; Cox, 1996). The specific preprocessing steps used were: (1) physiological motion correction, (2) 6-parameter rigid body motion correction, (3) spatial normalization to MNI space, (4) spatial smoothing with a 8 mm Gaussian kernel

(producing a final voxel size of 4 mm isotropic), and finally (5) the white matter and cerebrospinal fluid-related time-series were regressed from the time-series of each voxel. To correct for the effects of motion that are known to persist despite standard processing steps (e.g., Power et al., 2012) an additional motion-scrambling procedure was included at the end of our preprocessing pipeline (Anderson et al., 2014; Campbell et al., 2013). Using a conservative multivariate technique, time points that were outliers on both the six rigid-body motion parameter estimates and average fMRI BOLD signal were removed, and the BOLD signal was interpolated across using adjacent data points. This process minimizes the effects of motion-induced spikes in the BOLD signal without leaving sharp discontinuities due to the removal of outlying volumes (for details, see Campbell et al. (2013)).

2.2.3. Data analysis: Seed Partial Least Squares

The resting state data were analyzed using Seed-Partial Least Squares (seed-PLS) (McIntosh and Lobaugh, 2004; Krishnan et al., 2011), a multivariate analysis technique that can identify whole-brain patterns of activity related to the specific time-course of a predefined region or pair of regions. Seed-PLS does not require a priori contrasts typical of univariate techniques (e.g., subtraction method), and thus provides a data-driven approach to characterizing patterns of brain connectivity associated with specific seed regions. Furthermore, seed-PLS allows one to model the multivariate patterns of connectivity across multiple seeds simultaneously, providing an optimal technique to statistically compare whole-brain connectivity patterns associated with the left and right AG.

Similar to principal component analysis, PLS identifies a set of principal components or “latent variables” (LVs) that best account for the covariance in the data, but in the case of seed-PLS, these LVs are specifically calculated from a correlation matrix of the activity in the seeded region and correlations with all voxels in the brain. To produce the values used to create this correlation matrix, resting-state timecourses were artificially “blocked” by concatenating consecutive 5-volume sets to produce 46 “blocks” of 10 s each (excluding the first 5 TRs to allow for signal normalization). This procedure replicates the effect of low-pass filtering at .1 Hz, reducing temporal noise (Grigg and Grady, 2010a,b).

Next, we selected our seed regions located in the bilateral angular gyrus/posterior inferior parietal lobule: left AG ($X: -44, Y: -68, Z: 28$) and right AG ($X: 50, Y: -72, Z: 32$). We were interested in finding bilaterally defined regions in the AG that fell within the DMN and also responded to rich memory conditions. To accomplish this, we used the Neurosynth package (Yarkoni et al., 2011) to produce a reverse-inference map of the term “default”, FDR corrected at $p < .01$. This provided a map of brain regions preferentially related to the term “default” in previously published literature, including data from 627 separate studies during either task or rest, acting as a standard DMN template. Then, we produced another reverse-inference map of the term “autobiographical memory”, derived from 64 separate studies, and masked this autobiographical memory map with our DMN template. This provided a map of DMN regions that was also associated with autobiographical memory (see Fig. S1 in Supplementary data). We chose “autobiographical memory” as our reference point to find areas associated with mnemonic processing because of the complex and multimodal nature of autobiographical memories, known to engage bilateral AG (e.g., Elman et al., 2013; also, see meta-analyses in Andrews-Hanna et al. (2014)). As autobiographical memory retrieval engages both episodic memory and self-related/mentalizing processes (D’Argebeau et al., 2014; Rabin et al., 2010), each of which is mediated by separable subsystems of the DMN (Andrews-Hanna et al., 2010), we considered autobiographical memory most suitable to determine task-related nodes from both subsystems of the network. To identify our specific seeds, we applied anatomical masks of the

AG from the AAL atlas (Tzourio-Mazoyer et al., 2002) and determined the peak voxel within each AG to find the coordinates to use for our seeds. Furthermore, we used the same map to determine seed coordinates of the entire DMN for univariate analysis in Experiment 2 (see Section 2.3.4).

For each participant, we then extracted the mean signal from a $4 \times 4 \times 4$ mm³ voxel centered on the seed coordinates, per block. Then, the mean value for the seed was correlated, per block, with the mean signal from the remaining brain voxels, across subjects, creating a matrix of seed to whole-brain correlations (for a detailed example, see Krishnan et al. (2011)). Once these seed to whole-brain correlations were calculated, the subsequent correlation matrix was parsed into LVs using singular value decomposition (SVD), where each LV represented a spatial pattern of correlation, or functional connectivity, between seeded region(s) and the entire brain. Statistical significance of each LV as a whole was determined using a permutation test, using 500 permutations. This test determined whether the covariance accounted for by a specific LV was significantly different from a sampling distribution of 500 singular values derived from 500 random permutations of the data (for details, see Krishnan et al. (2011); McIntosh and Lobaugh (2004)). In addition, the contribution of each voxel to the identified spatial pattern in the brain was tested by submitting all voxel salience values (i.e., their contribution to an LV) to a bootstrap estimation of the standard errors (SEs; Efron, 1981) with 100 bootstraps. The bootstrap estimation procedure calculates how robustly each voxel contributed to the spatial pattern of a specific LV.

LVs calculated using PLS are orthogonal to one another, and may consist of clearly dissociable positive and negative dimensions. These dimensions, in seed-PLS, represent contrasting patterns of functional connectivity (i.e., the warm versus cold-colored regions seen in Fig. 1b). The reliability of each voxel’s association with either the positive or negative dimension of an LV was determined by their bootstrap ratio (BSR), which is calculated by dividing the voxel’s salience score by its standard error, and itself has a positive or negative value. It is important to note, however, that the positive and negative attributions themselves are arbitrary and do not mean activation or deactivation. Instead, the positive and negative dimensions simply reflect two distributions of voxels that covary in a similar pattern to one another. BSR ratio thresholds were selected as half of the maximum BSR for the peak region (not including the seeded region). For the first LV, peak voxels with a $BSR \geq \pm 25$ ($p < .0001$) were considered to contribute reliably to the LV. Similar to principal component analyses, the first LV accounts for the most covariance in the data, while all subsequent LVs account for progressively less covariance. Consequently, the maximum positive and minimum negative BSRs for the second LV were less extreme than that of the first, so peak voxels with a BSR of ± 7 ($p < .0001$) were considered to contribute reliably to this LV (for another example of this, see Campbell et al. (2013)). Significant clusters were defined as having at least 5 contiguous voxels. We report coordinates in MNI space (see Tables 1 and 2).

Measures of the degree to which each participant expressed each LV pattern were calculated by multiplying each voxel’s salience by the BOLD signal in the voxel, and summing over all brain voxels. The resulting measure, or *brain score*, was produced for each participant in each “block”, per LV. Functional connectivity (as reported in the seed correlation plots in Fig. 1) was assessed by correlating these brain scores with each seed’s activity per “block” and a bootstrap estimation procedure was used to calculate 95% confidence intervals around these correlations. Correlations and 95% confidence intervals for each block were then averaged to depict the general pattern of functional connectivity associated with a specific LV. Because the first LV accounts for the most covariance in the data, if there is a common network to which both seeds are strongly connected, it is likely that it would be

identified in the first LV. Unique patterns of whole brain functional connectivity that may potentially differentiate between the two seeds should be identified by subsequent LVs. We report the first two LVs from the analysis, as they were the only significant LVs that captured the DMN.

To assess differences in the strength of the functional connectivity between the left and right AG and the identified brain patterns, we used a non-parametric Wilcoxon signed-rank test to compare the correlations between the two seeds and the brain scores across the resting state “blocks” for the two LVs. The p values from these analyses were Bonferroni corrected to maintain family-wise error rates (i.e., two comparisons, thus $p=.025$). In sum, if the left and right AG covary in the same direction and to the same extent with the pattern of regions in an LV, then both the left and right AG contribute significantly to the same network of functionally connected regions. If the left and right AG, instead, covary significantly in opposite directions this would indicate laterality effects in the pattern of whole-brain functional connectivity associated with the AG.

2.3. Experiment 2

2.3.1. Participants

Data collected from 20 younger adults at the University of Toronto were included in this experiment. They ranged between 18 and 24 years of age ($M=21.3$, $SD=1.9$), with an average of 15.3 years of education ($SD=1.56$). Participants were healthy, and without history of psychiatric or neurological disorders, drug abuse, or systemic disease that could affect cerebral blood flow and/or cognitive functioning (e.g., cardiovascular disease, diabetes, or hypertension). All participants were right-handed, and with normal or corrected to normal vision. Written consent was acquired for each participant, prior to participation.

2.3.2. Procedure

Participants took part in a larger associative encoding scanning session that began with a six-minute resting scan. Instructions for the rest condition were simply to keep eyes closed, lie still, and relax without falling asleep. Participants then performed a series of face-house paired-associate encoding blocks, followed by a similar resting scan, which were not directly relevant to the present line of inquiry. After these task blocks, participants performed an unconstrained autobiographical-retrieval condition where they were instructed to close their eyes, lie still, and recall a personal past experience in as much detail as possible. Participants were told that whenever the event they were recalling “ended”, they should begin recalling another event, and continue doing so for the entire six-minute duration of the scan. Finally, participants were asked to complete a post-scan questionnaire indicating how well they complied with the task instructions. All participants stated that they had no difficulties following the instructions. As we were only interested in the connectivity pattern during the resting-state and unconstrained retrieval condition, which were unrelated to the remainder of the experiment, we only present results from these conditions.

2.3.3. Data acquisition and processing

Participants were tested using a Siemens Trio 3-T scanner at the Rotman Research Institute at the Baycrest Centre for Geriatric Care. A 3D MP-RAGE sequence was used to collect the T1-weighted structural scans ($TR=2000$ ms, $TE=2.63$ ms, flip angle= 9° , $FOV=25.6$ cm², 192×256 matrix, 160 slices of 1 mm thickness). Six-minutes of eyes-closed resting and retrieval were collected from each participant. Both functional runs were collected with a T2-weighted EPI sequence (180 volumes, $TR=2000$ ms, $TE=24$ ms, flip angle= 70° , $FOV=20$ cm², 64×64 matrix, 30 slices of 3.5 mm thickness, gap=.5 mm). As mentioned above, these functional runs were embedded within a larger

experiment, which is outside of the focus of the current report. All images were acquired using an oblique orientation to alleviate issues of signal drop-out in regions of the ventral medial prefrontal cortex – important to the larger experimental procedure. Instructions for the functional runs were presented using E-Prime software (version 2, Psychology Software Tools, Inc.) on a screen viewed by the participants through a mirror mounted in the head coil. Head movements were reduced by placing cushions inside the head coil. Physiological measures of pulse and breathing rate were obtained during the scanning session.

Data were preprocessed using an identical pipeline to that in Experiment 1 (see above).

2.3.4. Data analysis: univariate ROI-to-ROI functional connectivity

ROI-based correlational analyses were performed using the CONN toolbox (Whitfield-Gabrieli and Nieto-Castanon, 2012). ROIs were created at each node of the DMN. To determine the locations of these specific nodes, we used the Neurosynth package (Yarkoni et al., 2011) to produce two reverse-inference maps, one of the term “default” derived from 627 separate studies, and another of the term “autobiographical memory” derived from 64 separate studies (both FDR corrected at $p < .01$). We then masked our map of “autobiographical memory” with the one we derived using “default”, creating a map of DMN regions that were also associated with autobiographical memory (see Fig. S1 in Supplementary data). In order to define nodes comparable to those of a previously reported model of DMN subsystems (Andrews-Hanna et al., 2010), in addition to their bilateral counterparts, we used the AAL atlas (Tzourio-Mazoyer et al., 2002) to define anatomical masks of cortex that have been reported to contain nodes of the DMN. Then, within each of these anatomical masks, we used AFNI (Cox, 1996) to find clusters of at least 10 contiguous voxels from the “default”-masked “autobiographical memory” reverse-inference map. Peak voxels from within each of these clusters were then used to specify the exact coordinates to use for our ROIs. This procedure allowed us to define a total of 19 peak coordinates that roughly corresponded to previously reported DMN subsystems, task-related and bilaterally-defined, which we then included in the ROI-based correlation analyses through the CONN toolbox (for more details, see Table S1 in Supplementary data). The fMRI time-courses associated with each voxel within an ROI (8 mm sphere surrounding each seed coordinate) were then averaged to produce an ROI time-series, and then the mean time-series from each ROI was correlated with all of the others using bivariate correlations. The subsequent ROI-to-ROI connectivity matrices (calculated on a per-individual basis) were then entered into a GLM to produce group-based statistics.

We performed a between-source contrast where we forced a statistical comparison of connectivity between the left and right AG to see which nodes of the DMN showed preferential connectivity with these critical nodes. This analysis was run separately on the two conditions to produce a set of ROIs showing AG laterality effects in functional connectivity during rest and during retrieval. The interaction between conditions was also computed to reveal DMN regions showing a significant laterality effect (i.e., left > right, or right > left) that differed between rest and retrieval (i.e., rest > retrieval, or rest < retrieval). All correlations were false-discovery rate (FDR) corrected to $p < .05$ to correct for multiple comparisons.

Recent work has demonstrated that task performance preceding rest can influence the functional connectivity patterns observed during rest (Grigg and Grady, 2010a; Stevens et al., 2010; Tambini et al., 2010). In our design, the unconstrained retrieval condition always followed the encoding blocks, and thus performance on the encoding task could have affected connectivity patterns, confounding the effects of the unconstrained retrieval. To account for this, we performed an identical between source contrast of left and right AG connectivity across the rest scan at the beginning of the experiment with a resting scan collected

immediately following the encoding task, prior to our retrieval condition. This would reveal any laterality differences in AG connectivity with the DMN due to the performance of the encoding task. No significant differences were found for any of the 19 DMN regions included in the analysis, suggesting that a residual influence of the encoding task did not account for differences between the rest and retrieval conditions reported below (for further discussion, please see [Supplementary data](#)).

3. Results

3.1. Experiment 1 (multivariate functional connectivity including the whole brain)

The first two LVs produced by the seed-PLS analysis captured the relationship between the bilateral AG and the DMN,

collectively explaining $\sim 86\%$ of the summed squared covariance in the data. The first LV was significant, $p < .002$, and accounted for 83.64% of the covariance. To confirm that this pattern of connectivity corresponded to the DMN, clusters were compared to a reverse-inference map of the term “default”, FDR corrected at $p < .01$, produced using the Neurosynth package ([Yarkoni et al., 2011](#)). This provided a map of brain regions acting as a standard DMN template against which we compared our results. If at least 40% of voxels fell within this reverse-inference map, they were considered part of the DMN and marked with a “Y” in [Table 1](#). Overall, 72.6% of voxels in LV1 overlapped with the standard DMN template, suggesting that this LV represents the same network. This LV indeed identified all the principal regions of the canonical DMN, including the posterior cingulate cortex and the medial prefrontal cortex, alongside regions of the AG bilaterally surrounding our seeded regions (see [Fig. 1a](#); for overlap with Neurosynth DMN, see [Fig. S3](#) in [Supplementary data](#)). Regions of the

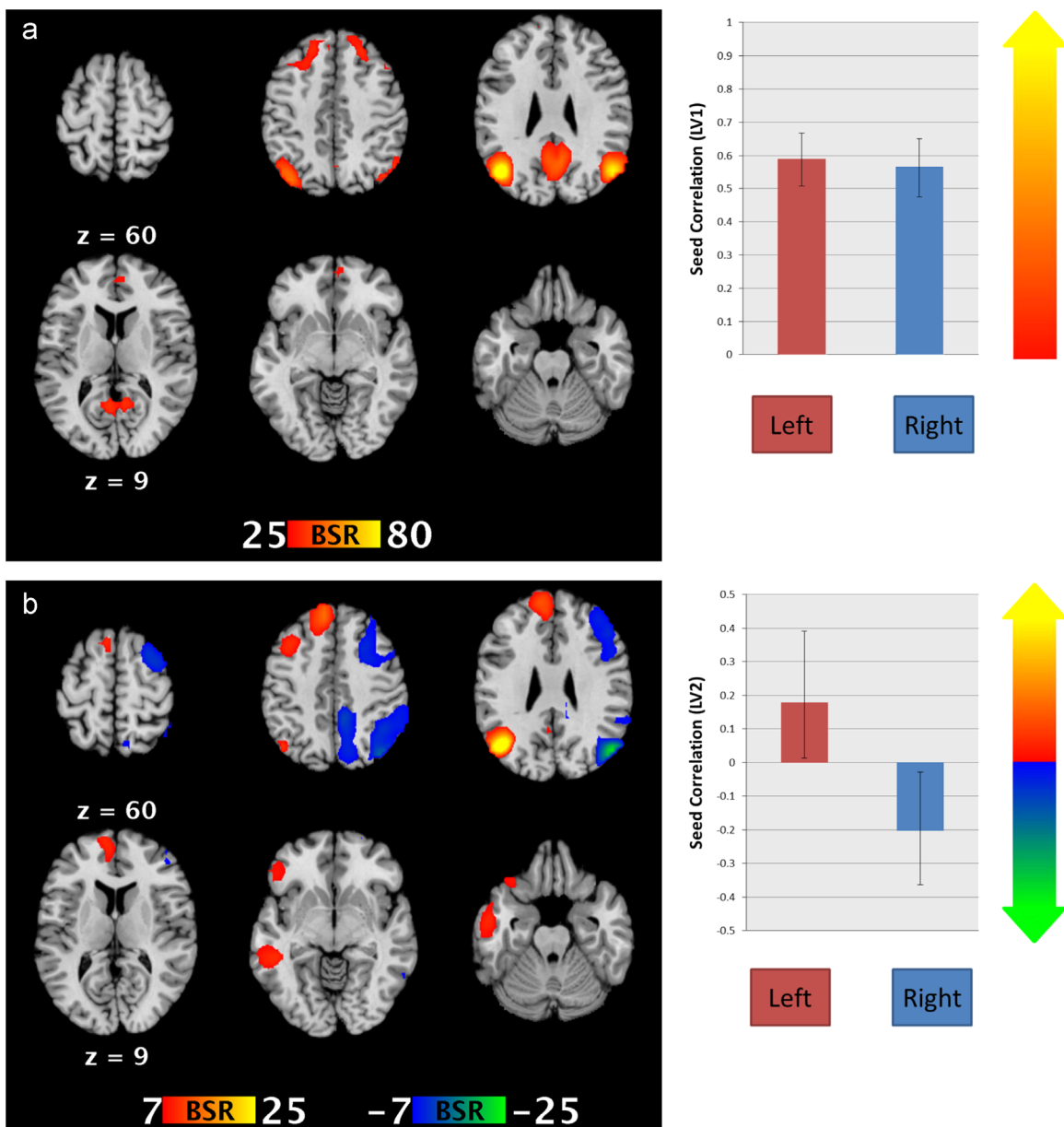


Fig. 1. Experiment 1: Multivariate functional connectivity pattern associated with Latent Variable 1 (1a) and Latent Variable 2 (1b). Positive seed correlation values indicate a positive association with the warm colored regions. Negative correlations indicate a positive association with the cool colored regions. Error bars represent 95% confidence intervals. (For interpretation of the references to color in this figure legend, the reader is referred to the web version of this article.)

Table 1

Results from seed PLS analysis for LV 1: brain regions showing significant functional connectivity with both the left and right AG seeds.

Peak region	DMN	x	y	z	BSR	# voxels
R Precuneus/posterior cingulate	Y	4	-64	28	49.71	463
L Superior frontal gyrus	Y	-20	32	48	37.73	214
R Superior frontal gyrus	Y	24	36	44	35.27	144
L Middle temporal gyrus	Y	-60	-28	-16	30.49	44
R Posterior inferior temporal gyrus	Y	64	-40	-16	29.98	15
R Ventromedial prefrontal cortex	Y	4	56	-16	29.87	124
R Anterior inferior temporal gyrus	N	64	-16	-24	28.21	5
R Superior frontal gyrus	N	16	64	4	27.24	8
R Anterior inferior temporal gyrus	N	60	0	-32	25.75	6

Clusters with bootstrap ratio of greater than ± 25 ($p < .0001$) and a cluster size of minimum 5 voxels are reported. Coordinates are in MNI space.

superior frontal gyri were also included in this LV as has been reported in other depictions of the DMN (e.g., Campbell et al., 2013), alongside regions of lateral temporal cortex (e.g., Andrews-Hanna et al., 2010). Few clusters reported in the LV did not correspond to regions of the DMN, but these clusters were relatively small, all under 8 voxels. Despite both the left and right AG contributing strongly to the same network, there was a significant difference in correlation strength between the left and right AG and this pattern of connectivity ($V=776$, $p=.009$), suggesting that the left AG connectivity contributed more to the DMN network as revealed by this first LV. However, when considering the largely overlapping averaged bootstrapped 95% CIs, this difference does not appear to be robust and may be attributable to the large sample size.

A second LV was also significant, $p < .002$, accounting for 2.21% of the summed squared covariance, and producing two clearly dissociable dimensions (see Fig. 1b and Table 2). The negative dimension represents a network of regions that included the right AG and extended into medial parietal cortex, middle and superior frontal gyri, and posterior inferior temporal cortex. Similar to the first LV, the positive dimension captured the core regions of the DMN, including the anterior medial prefrontal cortex and posterior cingulate cortex, as well as the left AG (for overlap with Neurosynth DMN, see Figs. S4 and S5 in Supplementary data). Despite the majority of the voxels in the positive dimension corresponding with the canonical DMN, two of the five significant clusters did not. These included regions of the left orbitofrontal cortex and middle frontal gyrus. Overall, 38.6% of all voxels in the positive dimension of LV2 overlap with the Neurosynth DMN, while the negative dimension has an overlap of 14.9%. Unlike LV1, which depicted the *commonality* across both seeds, LV2 shows a *difference* in whole brain connectivity between the left and right AG. The left AG showed significantly greater association with the positive dimension of LV2 (i.e., DMN), whereas the right AG showed a significant connectivity with the negative dimension instead ($V=1081$, $p < .0001$), with clearly non-overlapping averaged 95% CIs. Therefore, in a small but reliable portion of the variance, we find a laterality effect in connectivity at rest, in which the left AG is better connected with the DMN than the right. It is important to note that the second LV is wholly orthogonal to the first; therefore, the left preference in connectivity only appears after accounting for the covariance associated with the commonality in right/left AG connectivity with the DMN.

Table 2

Results from seed PLS analysis for LV 2: brain regions showing significant differential functional connectivity between the left (positive BSR) and right (negative BSR) AG seeds.

Peak region	DMN	x	y	z	BSR	# voxels
L Dorsomedial prefrontal cortex	Y	-8	40	48	15.58	462
L Orbitofrontal cortex	N	-44	36	-16	12.38	174
L Inferior temporal gyrus	Y	-52	-4	-28	10.64	79
L Middle frontal gyrus	N	-36	20	44	10.53	27
L Precuneus/posterior cingulate cortex	Y	-4	-56	24	7.72	41
R Middle frontal gyrus	N	28	16	48	-13.49	469
R Precuneus/posterior cingulate cortex	N	12	-40	40	-12.56	239
R Inferior temporal gyrus	N	60	-52	-16	-8.55	20

Clusters with bootstrap ratio of greater than ± 7 ($p < .0001$) and a cluster size of minimum 5 voxels are reported. Coordinates are in MNI space.

3.2. Experiment 2 (univariate functional connectivity restricted to DMN regions)

At rest, the between-source contrast revealed that the left AG showed significantly greater connectivity, relative to the right, with the majority of DMN nodes (see Fig. 2). The regions showing this left preference include the left temporoparietal junction, dorsomedial and ventromedial prefrontal cortex, left lateral temporal cortex and regions of the medial temporal lobe (FDR, $p < .05$) (see Table 3). No DMN nodes showed preferential connectivity with the right AG during rest. A left laterality effect in DMN connectivity during rest replicates the findings of the second LV from the previous seed-PLS analysis, now demonstrated in two independent samples while using different analysis techniques.

Interestingly, when this analysis was run on the unconstrained retrieval data, a different pattern of results emerged (see Fig. 3). The left AG continued to show significantly greater connectivity (relative to the right AG) with some regions of the DMN, including the medial prefrontal cortices, left temporoparietal junction, left lateral temporal cortex and dorsal AG (FDR, $p < .05$). However, the right AG showed significantly greater connectivity (relative to the left AG) with the right parahippocampal cortex and retrosplenial cortex (FDR, $p < .05$) (see Table 4).

Furthermore, when we examined the differences between the rest and unconstrained retrieval conditions (i.e., by contrasting retrieval – rest, to show those regions with laterality effects for connectivity during retrieval when controlling for connectivity at rest), the right AG showed a trend towards better connectivity, relative to the left AG, with left posterior parahippocampal cortex (FDR, $p .06$). Both right parahippocampal and retrosplenial cortex, where a significant right AG preference was observed during retrieval, showed a trend towards significance but did not survive FDR correction (see Table 5).

These results suggest that the left AG is better connected with some regions of the DMN, even during directed retrieval, but they are non-MTL regions. The right AG, on the other hand, specifically shows better connectivity with regions of the MTL in the DMN during retrieval.

4. Discussion

To achieve a better understanding of the laterality effects in recruitment of AG during episodic memory retrieval, the present study examined the connectivity between the left and right AG with the DMN, a large-scale network showing reliable recruitment during the retrieval of episodic memories (Andrews-Hanna et al.,

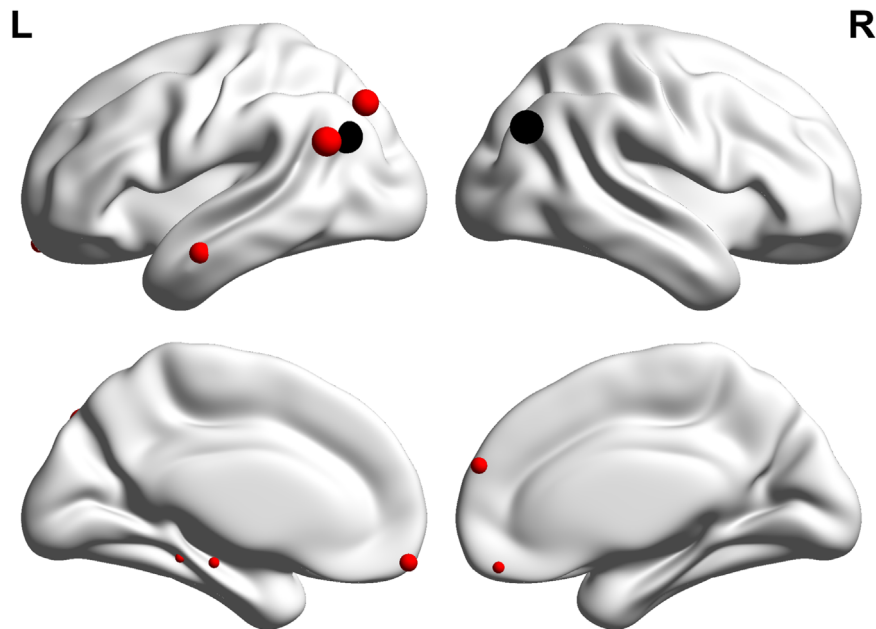


Fig. 2. Experiment 2: Univariate seed connectivity pattern associated with the resting condition. Red spheres=better connectivity with the left angular gyrus. Black spheres=seed regions. Size of node represents the magnitude of correlation. (For interpretation of the references to color in this figure legend, the reader is referred to the web version of this article.)

Table 3

Results from the univariate functional connectivity analysis on resting data (Experiment 2): regions showing a significant laterality preference at rest.

	Region	Beta	<i>t</i>	<i>p</i> -FDR
L	Temporoparietal junction	.43	7.15	.000015
L	Dorsal angular gyrus	.38	5.76	.00013
L	Lateral temporal cortex	.30	5.00	.00045
L	Ventromedial prefrontal cortex	.23	4.38	.0012
R	Dorsomedial prefrontal cortex	.21	3.80	.0041
L	Posterior cingulate cortex	.19	3.32	.01
R	Ventromedial prefrontal cortex	.13	2.70	.033
L	Posterior parahippocampal cortex	.09	2.66	.033
L	Hippocampus	.11	2.57	.034

Positive beta values indicate better connectivity between that region and the left AG seed.

2014). The primary questions the present study addressed were as follows: (1) Do both the left and right AG contribute to the DMN at rest? (2) If there are differences in connectivity with the DMN at rest, in which DMN subregions are they present? (3) How do these laterality differences change during active episodic retrieval?

Using a seed-PLS approach, we found, in Experiment 1, that the left and right AG showed a common whole-brain connectivity pattern with the rest of the DMN. This answers our first question, suggesting that the left and right AG *both* contribute to the DMN at rest. Critically, this commonality accounts for most of the variance. Once this commonality is taken into account, however, a reliable laterality effect can be found, in which the left AG shows better connectivity with a subset of the DMN. Results from Experiment 2 complement these findings. The univariate connectivity analysis at rest revealed better connectivity between the left AG and a wide array of nodes of the DMN. The right AG did not show any significant laterality effects in DMN connectivity relative to the left at rest. This finding replicates the left asymmetry from Experiment 1 and answers our second question, suggesting that when the left bias is tested directly, it appears consistently across most DMN subregions.

Overall, these resting data suggest that both the left and right AG are coupled with DMN regions in the absence of explicit task

demands, but the left AG appears to have stronger connectivity with this network. Considering that activity in the left AG has been reported more reliably than activity in the right during active episodic retrieval (Levy, 2012), the differences we observe in functional connectivity may represent better intrinsic coupling between the left AG and the DMN (as a whole), and perhaps this difference contributes to the greater likelihood of finding left lateralized activations.

In contrast, during active episodic retrieval, a different pattern emerged. When the univariate contrast was run on DMN connectivity, the left laterality effect remained, but was restricted to the non-MTL regions of the DMN. By contrast, the right AG showed significantly greater connectivity with MTL regions. Furthermore, when we tested the interaction (i.e., regions showing laterality effects during retrieval after controlling for connectivity at rest), the left AG no longer showed any regions with preferential connectivity. The right AG, however, continued to show trends towards greater connectivity with the parahippocampal cortex relative to the left AG. Thus, to address our last question, retrieval appears to alter laterality effects in AG-DMN connectivity primarily in the right AG, which showed preferential connectivity with the parahippocampal cortex; the greater connectivity of the left AG with non-MTL regions of the DMN seen at rest was unchanged during retrieval.

4.1. Bilateral contributions to episodic retrieval

These findings suggest an interesting difference between the left and right AG. During rest, both the left and right AG show robust functional connectivity with the DMN, but a small and reliable bias can be seen towards the left AG. This bias was present both in the multivariate analysis in Experiment 1 and the univariate analysis in Experiment 2, in two separate samples. The slight left preference receives support from other studies exploring the constituents of the DMN at rest (Fornito et al., 2012; Andrews-Hanna et al., 2010). Seed-PLS, however, provides a unique opportunity to characterize the similarity, as well as the difference, in patterns of connectivity between these two seeds, which has not, to our knowledge, been directly addressed in the literature.

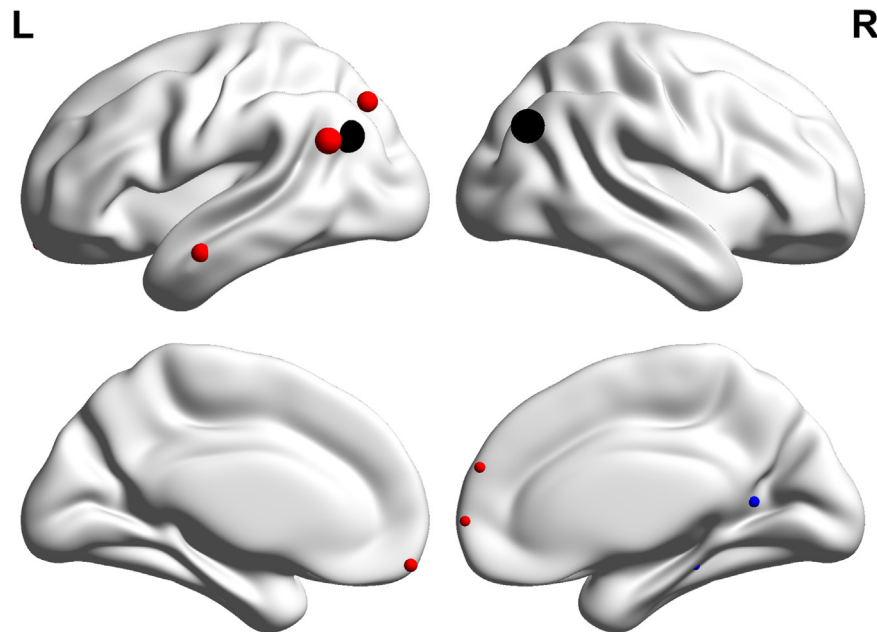


Fig. 3. Experiment 2: Univariate seed connectivity pattern associated with the retrieval condition. Blue colored spheres=better connectivity with the right angular gyrus. Red spheres=better connectivity with the left angular gyrus. Black spheres=seed regions. Size of node represents the magnitude of correlation. (For interpretation of the references to color in this figure legend, the reader is referred to the web version of this article.)

Table 4

Results from the univariate functional connectivity analysis on retrieval data (Experiment 2): regions showing a significant laterality preference during episodic retrieval.

	Region	Beta	<i>T</i>	<i>p</i> -FDR
L	Temporoparietal junction	.40	6.45	.000059
L	Lateral temporal cortex	.31	5.88	.0001
L	Dorsal angular gyrus	.32	5.13	.00034
L	Ventromedial prefrontal cortex	.22	4.77	.00057
R	Anterior medial prefrontal cortex	.18	4.28	.0014
R	Dorsomedial prefrontal cortex	.19	4.15	.0015
R	Retrosplenial cortex	-.19	-3.95	.0021
R	Parahippocampal cortex	-.17	-3.30	.008
L	Posterior cingulate cortex	.18	2.90	.017

Positive beta values indicate better connectivity between that region and the left AG seed. Negative beta values indicate better connectivity with the right AG seed.

Table 5

Results from the univariate functional connectivity analysis examining laterality preference for retrieval over rest (Experiment 2).

	Region	Beta	<i>T</i>	<i>p</i> -uncorr.	<i>p</i> -FDR
L	Posterior parahippocampal cortex	-.17	-3.32	.0036	.061
R	Parahippocampal cortex	-.17	-2.67	.015	.12
R	Retrosplenial cortex	-.12	-2.50	.022	.12

Negative beta values indicate better connectivity with the right AG seed.

Interestingly, we observed that this left bias during rest extended to regions of the MTL in Experiment 2. During active retrieval, however, the right AG showed greater connectivity with regions of the MTL than the left.

Considering the MTL is known to be critical for episodic memory processes (Moscovitch, 1992; Preston and Eichenbaum, 2013; Ranganath, 2010; Scoville and Milner, 1957; Shimamura, 2010), preferential functional connectivity between these two regions supports the notion that the right AG may be actively contributing to episodic memory alongside the MTL. In Experiment 2, this relationship was specific to retrieval of episodic memory and not to rest, further suggesting that the connectivity between the

MTL and the right AG are task-related, and contributing in some degree to the process of episodic retrieval. This interpretation is consistent with early work demonstrating a bilateral recruitment of the AG during retrieval (e.g., Shannon and Buckner, 2004), and, more recently, with studies emphasizing bilateral recruitment when retrieval is detail-rich or recollection-based. For example, personally familiar scenes in a recognition task were shown to produce robust bilateral AG recruitment in healthy young adults (Elman et al., 2013). In patients, bilateral damage to the PPC (including the AG) has been shown to produce more severe memory impairments than unilateral damage, regardless of the affected hemisphere (Simons et al., 2010; for reviews, see Berryhill (2012) and Schoo et al. (2011)). A comprehensive set of lesion studies recently conducted by Ben-Zvi et al. (2015) demonstrates that greater damage to the right AG is associated with poorer performance on a multimodal source memory task. Finally, recent neuroimaging work demonstrates that AG recruitment during episodic retrieval may be left lateralized when contrasting correctly recognized old against new items, but this left bias diminishes when contrasting recollected against familiar items (Elward and Rugg, 2014). A contrast comparing recollected items versus familiar ones is an optimal assessment of memory detail, and does not include the overall memory effect present within an old-new contrast, so the loss of the left bias would suggest a more robust involvement of the right AG during rich recollection of details. Therefore, although an overall left laterality effect may be present in the episodic retrieval literature, functional connectivity suggests that the right AG is also involved, perhaps especially during rich episodic retrieval or recollection.

4.2. Differential connectivity profiles and functional implications

Although both left and right AG contribute to episodic memory, interesting distinctions emerged when their patterns of functional connectivity within the DMN were probed. During retrieval, the left AG showed significantly greater connectivity with the non-MTL regions of the DMN, including regions of the medial prefrontal cortex, lateral temporal cortex, and temporoparietal junction. A very similar network of regions, described as a dorsomedial

prefrontal subsystem, was reported by Andrews-Hanna et al. (2010) when using functional connectivity at rest and graph theoretic methods to parse the DMN into its subcomponents. This subsystem was associated with processes of theory-of-mind and social cognition, rather than with the memory processes thought to be supported by an MTL-centric subsystem of the DMN (Andrews-Hanna et al., 2010, 2014). Furthermore, in a recent study, Flegal et al. (2014) showed that regions of the dorsomedial subsystem supported confident retrieval of word pairs, irrespective of whether their encoding context was reinstated, suggesting that the dorsomedial subsystem may also play a role in the subjective nature of confident recognition rather than the retrieval of the objective encoding context. At first, this may seem inconsistent with the previous studies of episodic retrieval demonstrating that both subjective measures of recollection (e.g., remember-know) and objective measures (e.g., source memory, where the accuracy of retrieved details can be determined) recruit the left AG (e.g., Frithsen and Miller, 2014). However, retrieval or recollection of objective details is almost always accompanied by the subjective feeling of confidence in those details (Yonelinas, 2001), thus making the individual contributions of the objective and subjective aspects of recollection difficult to disentangle experimentally. One possibility is that the left AG activity may track the subjective aspects of recollection even during the performance of objective memory tests. Previous work demonstrating that false memories (i.e., false alarms during recognition) also recruit the left AG provides support for this claim (Wheeler and Buckner, 2003; for discussion, see Cabeza et al. (2012)). Furthermore, a recent meta-analysis of subjective confidence ratings in mnemonic tasks demonstrated that the left AG was amongst the most reliable brain regions to be activated for high confidence responses (White et al., 2014). Taken together with evidence of reduced connectivity of the left AG with regions of the MTL as observed in present study, our data suggest that the left laterality effect in AG recruitment often reported in the literature may actually reflect increased subjective confidence, more so than the objective recollection of details (e.g., Hower et al., 2014; Simons et al., 2010; Yazar et al., 2014).

In the present study, the right AG, unlike the left, showed strong connectivity with regions of the MTL, including the bilateral parahippocampal cortex, and right retrosplenial cortex. These regions of the MTL correspond to some components of the MTL-centric subsystem of the DMN, reported by Andrews-Hanna et al. (2010). This subsystem was thought largely to support the DMN's contribution to episodic memory retrieval. Interestingly, Flegal et al. (2014) reported that activation of the parahippocampal cortex and hippocampi increased specifically when the encoding context was successfully reinstated during retrieval of a word pair, or in other words, when specific details from the encoding context were successfully retrieved. Our observation that the right AG is integrated better than the left AG to the MTL subsystem, suggests that the right AG, more than the left, supports the objective retrieval of episodic memory details.

Current theoretical models of the contributions of the AG, and posterior parietal cortex more generally, to episodic memory have largely ignored the role of the right AG, and often rely on communication between the hippocampus and left AG (Cabeza et al., 2012; Ciaramelli et al., 2010; Vilberg and Rugg, 2008; Shimamura, 2011; Wagner et al., 2005). Both structural and functional connections between the hippocampus and the left AG have been reported in the literature (Vincent et al., 2006; Uddin et al., 2010), providing neurobiological support for communication between these regions. Our data do not suggest that there is no communication between the left AG and the MTL, only that it is less than that of the right AG during retrieval. Similarly, it is only in comparison with the right AG that the left assumes a dominant role in accessing the subjective aspects of recollection, as supported by its

increased connectivity with the dorsomedial subsystem during retrieval, and by previous work associating it with confidence ratings. Therefore, bilateral AG may support the retrieval of objective aspects of episodic memories through direct and indirect connections with the MTL, whereas the specific left laterality effect observed in the literature may be more related to subjective confidence.

4.3. Conclusion

In summary, our results suggest that both left and right AG are strongly connected components of the DMN and are engaged during retrieval. During the performance of an unconstrained retrieval task, the left and right AG show differential connectivity within the subsystems of the DMN that may support separable aspects of episodic retrieval. Though this specific proposal requires further investigation, evidence of networks shifting and reconfiguring depending on the demands of the task and the information being processed is consistent with a component process approach to memory (Moscovitch, 1992; Cabeza and Moscovitch, 2013) in which different components of large networks form temporary alliances. These constitute subnetworks that operate to meet the requirements of the tasks at hand, and implement them successfully.

Acknowledgments

We would like to thank Nick Diamond and Vincent Man for many helpful discussions regarding the project. The research was funded by the Natural Sciences and Engineering Research Council of Canada, (Canada) individual fellowship to BB, an NSERC Grant (A8347) to MM, and a Canadian Institutes for Health Research (CIHR) Grant (MOP14036) to CG. We also would like to thank the following people for their generosity in support of the imaging centre at Baycrest: Jack & Anne Weinbaum, Sam & Ida Ross, Joseph & Sandra Rotman.

Appendix A. Supplementary material

Supplementary data associated with this article can be found in the online version at <http://dx.doi.org/10.1016/j.neuropsychologia.2015.11.004>.

References

- Aggleton, J.P., 2012. Multiple anatomical systems embedded within the primate medial temporal lobe: implications for hippocampal function. *Neurosci. Biobehav. Rev.* 36 (7), 1579–1596. <http://dx.doi.org/10.1016/j.neubiorev.2011.09.005>.
- Aggleton, J.P., Brown, M.W., 2006. Interleaving brain systems for episodic and recognition memory. *Trends Cogn. Sci.* 10 (10), 455–463. <http://dx.doi.org/10.1016/j.tics.2006.08.003>.
- Anderson, J., Campbell, K., Amer, T., Grady, C.L., Hasher, L., 2014. Timing is everything: age differences in the cognitive control network are modulated by time of day. *Psychol. Aging* 29 (3), 648–657. <http://psycnet.apa.org/psycinfo/2014-27996-001/>.
- Andrews-Hanna, J.R., Saxe, R., Yarkoni, T., 2014. Contributions of episodic retrieval and mentalizing to autobiographical thought: evidence from functional neuroimaging, resting-state connectivity, and fMRI meta-analyses. *NeuroImage* 91, 1–12. <http://dx.doi.org/10.1016/j.neuroimage.2014.01.032>.
- Andrews-Hanna, J.R., Reidler, J.S., Sepulcre, J., Poulin, R., Buckner, R.L., 2010. Functional-anatomic fractionation of the brain's default network. *Neuron* 65 (4), 550–562. <http://dx.doi.org/10.1016/j.neuron.2010.02.005>.
- Benoit, R.G., Schacter, D.L., 2015. Specifying the core network supporting episodic simulation and episodic memory by activation likelihood estimation. *Neuropsychologia* 75, 450–457. <http://dx.doi.org/10.1016/j.neuropsychologia.2015.06.034>.
- Ben-Zvi, S., Soroker, N., Levy, D.A., 2015. Parietal lesion effects on cued recall

- following pair associate learning. *Neuropsychologia* 73, 176–194. <http://dx.doi.org/10.1016/j.neuropsychologia.2015.05.009>.
- Berryhill, M.E., 2012. Insights from neuropsychology: pinpointing the role of the posterior parietal cortex in episodic and working memory. *Front. Integr. Neurosci.* 6, 1–12. <http://dx.doi.org/10.3389/fnint.2012.00031>.
- Cabeza, R., Moscovitch, M., 2013. Memory systems, processing modes, and components: functional neuroimaging evidence. *Perspect. Psychol. Sci.* 8 (1), 49–55. <http://dx.doi.org/10.1177/1745691612469033>.
- Cabeza, R., Ciaramelli, E., Moscovitch, M., 2012. Cognitive contributions of the ventral parietal cortex: an integrative theoretical account. *Trends Cogn. Sci.* 16 (6), 338–352. <http://dx.doi.org/10.1016/j.tics.2012.04.008>.
- Campbell, K., Grigg, O., Saverino, C., Churchill, N., Grady, C., 2013. Age differences in the intrinsic functional connectivity of default network subsystems. *Front. Hum. Neurosci.* 5, 73. <http://dx.doi.org/10.3389/fnagi.2013.00073>.
- Ciaramelli, E., Grady, C.L., Moscovitch, M., 2008. Top-down and bottom-up attention to memory: a hypothesis (AtOM) on the role of the posterior parietal cortex in memory retrieval. *Neuropsychologia* 46 (7), 1828–1851. <http://dx.doi.org/10.1016/j.neuropsychologia.2008.03.022>.
- Ciaramelli, E., Grady, C., Levine, B., Ween, J., Moscovitch, M., 2010. Top-down and bottom-up attention to memory are dissociated in posterior parietal cortex: Neuroimaging and neuropsychological evidence. *The Journal of Neuroscience* 30 (14), 4943–4956. <http://dx.doi.org/10.1523/JNEUROSCI.1209-09.2010>.
- Cole, M.W., Bassett, D.S., Power, J.D., Braver, T.S., Petersen, S.E., 2014. Intrinsic and task-evoked network architectures of the human brain. *Neuron* 83 (1), 238–251. <http://dx.doi.org/10.1016/j.neuron.2014.05.014>.
- Cox, R.W., 1996. AFNI: software for analysis and visualization of functional magnetic resonance 25 neuroimages. *Comput. Biomed. Res.* 29, 162–173.
- D'Argembeau, A., Cassol, H., Phillips, C., Baetee, E., Salmon, E., Van der Linden, M., 2014. Brains creating stories of selves: the neural basis of autobiographical reasoning. *Soc. Cogn. Affect. Neurosci.* 9 (5), 646–652. <http://dx.doi.org/10.1093/scan/nst028>.
- Damasio, A.R., Graff-Radford, N.R., Eslinger, P.J., Damasio, H., Kassel, N., 1985. Amnesia following basal forebrain lesions. *Arch. Neurol.* 42 (3), 263–271. <http://dx.doi.org/10.1001/archneur.1985.04060030081013>.
- Daselaar, S.M., Prince, S.E., Dennis, N.A., Hayes, S.M., Kim, H., Cabeza, R., 2009. Posterior midline and ventral parietal activity is associated with retrieval success and encoding failure. *Front. Hum. Neurosci.* 3, 13. <http://dx.doi.org/10.3389/fnro.09.013.2009>.
- Efron, B., 1981. Nonparametric estimates of standard error: the jackknife, the bootstrap, and 32 other methods. *Biometrika* 68, 589–599.
- Elman, J.A., Cohn-Sheehy, B.I., Shimamura, A.P., 2013. Dissociable parietal regions facilitate successful retrieval of recently learned and personally familiar information. *Neuropsychologia* 51 (4), 573–583. <http://dx.doi.org/10.1016/j.neuropsychologia.2012.12.013>.
- Elward, R., Rugg, M.D., 2014. The lateral distribution of recollection effects in posterior parietal cortex. *Program No. 172.11.2014*. Neuroscience Meeting Planner. Society for Neuroscience, Washington, DC. Online.
- Flegel, K., Marín-Gutiérrez, A., Ragland, J.D., Ranganath, C., 2014. Brain mechanisms of successful recognition through retrieval of semantic context. *J. Cogn. Neurosci.* 26, 1–11. <http://dx.doi.org/10.1162/jocn.2014.0185109>.
- Fornito, A., Harrison, B.J., Zalesky, A., Simons, J.S., 2012. Competitive and cooperative dynamics of large-scale brain functional networks supporting recollection. *Proc. Natl. Acad. Sci.* 109 (31), 12788–12793. <http://dx.doi.org/10.1073/pnas.1204185109>.
- Foster, B.L., Rangarajan, V., Shirer, W.R., Parvizi, J., 2015. Intrinsic and task-dependent coupling of neuronal population activity in human parietal cortex. *Neuron* 86 (2), 578–590. <http://dx.doi.org/10.1016/j.neuron.2015.03.018>.
- Frithsen, A., Miller, M.B., 2014. The posterior parietal cortex: comparing remember/know and source memory tests of recollection and familiarity. *Neuropsychologia* 61, 1–14. <http://dx.doi.org/10.1016/j.neuropsychologia.2014.06.011>.
- Gilmore, A.W., Nelson, S.M., McDermott, K.B., 2015. A parietal memory network revealed by multiple MRI methods. *Trends Cogn. Sci.* 19, 1–10. <http://dx.doi.org/10.1016/j.tics.2015.07.004>.
- Grigg, O., Grady, C.L., 2010a. Task-related effects on the temporal and spatial dynamics of resting-state functional connectivity in the default network. *PLoS One* 5 (10), 1–12. <http://dx.doi.org/10.1371/journal.pone.0013311>.
- Grigg, O., Grady, C.L., 2010b. The default network and processing of personally relevant information: converging evidence from task-related modulations and functional connectivity. *Neuropsychologia* 48 (13), 3815–3823. <http://dx.doi.org/10.1016/j.neuropsychologia.2010.09.007>.
- Hower, K.H., Wixted, J., Berryhill, M.E., Olson, I.R., 2014. Impaired perception of mnemonic oldness, but not mnemonic newness, after parietal lobe damage. *Neuropsychologia* 56, 409–417. <http://dx.doi.org/10.1016/j.neuropsychologia.2014.02.014>.
- Huijbers, W., Schultz, A.P., Vannini, P., McLaren, D.G., Wigman, S.E., Ward, A.M., 2012. The encoding/retrieval flip: interactions between memory performance and memory stage and relationship to intrinsic cortical networks. *J. Cogn. Neurosci.* 25 (7), 1–17.
- Humphreys, G.F., Lambon Ralph, M.A., 2014. Fusion and fission of cognitive functions in the human parietal cortex. *Cereb. Cortex* 25, 3547–3560. <http://dx.doi.org/10.1093/cercor/bhu198>.
- Jaeger, A., Konkel, A., Dobbins, I.G., 2013. Unexpected novelty and familiarity orienting responses in lateral parietal cortex during recognition judgment. *Neuropsychologia* 51 (6), 1061–1076. <http://dx.doi.org/10.1016/j.neuropsychologia.2013.02.018>.
- Krishnan, A., Williams, L.J., McIntosh, A.R., Abdi, H., 2011. Partial Least Squares (PLS) methods for neuroimaging: a tutorial and review. *NeuroImage* 56 (2), 455–475. <http://dx.doi.org/10.1016/j.neuroimage.2010.07.034>.
- Levy, D.A., 2012. Towards an understanding of parietal mnemonic processes: some conceptual guideposts. *Front. Integr. Neurosci.* 6, 41. <http://dx.doi.org/10.3389/fnint.2012.00041>.
- Maguire, E.A., 2001. Neuroimaging studies of autobiographical event memory. *Philos. Trans. R. Soc. Lond. Ser. B Biol. Sci.* 356, 1441–1451. <http://dx.doi.org/10.1098/rstb.2001.0944>.
- McCormick, C., Protzner, A.B., Barnett, A.J., Cohn, M., Valiante, T.A., McAndrews, M.P., 2014. Linking DMN connectivity to episodic memory capacity: what can we learn from patients with medial temporal lobe damage. *NeuroImage Clin.* 5, 188–196. <http://dx.doi.org/10.1016/j.nicl.2014.05.008>.
- McDermott, K.B., Szpunar, K.K., Christ, S.E., 2009. Laboratory-based and autobiographical retrieval tasks differ substantially in their neural substrates. *Neuropsychologia* 47 (11), 2290–2298. <http://dx.doi.org/10.1016/j.neuropsychologia.2008.12.025>.
- McIntosh, A.R., Lobaugh, N.J., 2004. Partial least squares analysis of neuroimaging data: applications and advances. *NeuroImage* 23 (Suppl 1), S250–S263. <http://dx.doi.org/10.1016/j.neuroimage.2004.07.020>.
- Montaldi, D., Mayes, A.R., 2010. The role of recollection and familiarity in the functional differentiation of the medial temporal lobes. *Hippocampus* 20 (11), 1291–1314. <http://dx.doi.org/10.1002/hipo.20853>.
- Moscovitch, M., 1992. Memory and working-with-memory: a component process model based on modules and central systems. *J. Cogn. Neurosci.* 4 (3), 257–267.
- Nelson, S.M., Cohen, A.L., Power, J.D., Wig, G.S., Miezin, F.M., Wheeler, M.E., Petersen, S.E., 2010. A parcellation scheme for human left lateral parietal cortex. *Neuron* 67 (1), 156–170. <http://dx.doi.org/10.1016/j.neuron.2010.05.025>.
- Power, J.D., Barnes, K.A., Snyder, A.Z., Schlaggar, B.L., Petersen, S.E., 2012. Spurious but systematic correlations in functional connectivity MRI networks arise from subject motion. *NeuroImage* 59 (3), 2142–2154. <http://dx.doi.org/10.1016/j.neuroimage.2011.10.018>.
- Preston, A.R., Eichenbaum, H., 2013. Interplay of hippocampus and prefrontal cortex in memory. *Curr. Biol.* 23 (17), R764–R773. <http://dx.doi.org/10.1016/j.cub.2013.05.041>.
- Rabin, J.S., Gilboa, A., Stuss, D.T., Mar, R.A., Rosenbaum, R.S., 2010. Common and unique neural correlates of autobiographical memory and theory of mind. *J. Cogn. Neurosci.* 22 (6), 1095–1111. <http://dx.doi.org/10.1162/jocn.2009.21344>.
- Ranganath, C., 2010. A unified framework of the functional organization of the medial temporal lobes and the phenomenology of episodic memory. *Hippocampus* 20 (11), 1263–1290. <http://dx.doi.org/10.1002/hipo.20852>.
- Rugg, M.D., Vilberg, K.L., 2013. Brain networks underlying episodic memory retrieval. *Curr. Opin. Neurobiol.* 23 (2), 255–260. <http://dx.doi.org/10.1016/j.conb.2012.11.005>.
- Schoo, L.A., van Zandvoort, M.J.E., Biessels, G.J., Kappelle, L.J., Postma, A., de Haan, E.H.F., 2011. The posterior parietal paradox: why do functional magnetic resonance imaging and lesion studies on episodic memory produce conflicting results? *J. Neuropsychol.* 5 (Pt 1), 15–38. <http://dx.doi.org/10.1348/174866410x504059>.
- Scoville, W.B., Milner, B., 1957. Loss of recent memory after bilateral hippocampal lesions. *J. Neurol. Neurosurg. Psychiatry* 20, 11–21. <http://jnnp.bmj.com/content/20/1/11.short>.
- Seghier, M.L., 2013. The angular gyrus: multiple functions and multiple subdivisions. *Neurosci.* 19 (1), 43–61. <http://dx.doi.org/10.1177/1073858412440596>.
- Shannon, B.J., Buckner, R.L., 2004. Functional-anatomic correlates of memory retrieval that suggest nontraditional processing roles for multiple distinct regions within posterior parietal cortex. *J. Neurosci.* 24 (45), 10084–10092. <http://dx.doi.org/10.1523/JNEUROSCI.2625-04.2004>.
- Shimamura, A.P., 2010. Hierarchical relational binding in the medial temporal lobe: the strong get stronger. *Hippocampus* 20, 1206–1216. <http://dx.doi.org/10.1002/hipo.20856>.
- Shimamura, A.P., 2011. Episodic retrieval and the cortical binding of relational activity. *Cogn. Affect. Behav. Neurosci.* 11 (3), 277–291. <http://dx.doi.org/10.3758/s13415-011-0031-4>.
- Shimamura, A.P., 2014. Remembering the past: neural substrates underlying episodic encoding and retrieval. *Curr. Dir. Psychol. Sci.* 23 (4), 257–263. <http://dx.doi.org/10.1177/0963721414536181>.
- Simons, J.S., Peers, P.V., Mazuz, Y.S., Berryhill, M.E., Olson, I.R., 2010. Dissociation between memory accuracy and memory confidence following bilateral parietal lesions. *Cereb. Cortex* 20 (2), 479–485. <http://dx.doi.org/10.1093/cercor/bhp116>.
- Skinner, E.L., Fernandes, M.A., 2007. Neural correlates of recollection and familiarity: a review of neuroimaging and patient data. *Neuropsychologia* 45 (10), 2163–2179. <http://dx.doi.org/10.1016/j.neuropsychologia.2007.03.007>.
- Spaniol, J., Davidson, P.S.R., Kim, A.S.N., Han, H., Moscovitch, M., Grady, C.L., 2009. Event-related fMRI studies of episodic encoding and retrieval: meta-analyses using activation likelihood estimation. *Neuropsychologia* 47 (8–9), 1765–1779. <http://dx.doi.org/10.1016/j.neuropsychologia.2009.02.028>.
- Spreng, R.N., Mar, R.A., Kim, A.S.N., 2009. The common neural basis of autobiographical memory, prospection, navigation, theory of mind, and the default mode: a quantitative meta-analysis. *J. Cogn. Neurosci.* 21 (3), 489–510. <http://dx.doi.org/10.1162/jocn.2008.21029>.
- Stevens, W.D., Buckner, R.L., Schacter, D.L., 2010. Correlated low-frequency BOLD fluctuations in the resting human brain are modulated by recent experience in category-preferential visual regions. *Cereb. Cortex* 20, 1997–2006. <http://dx.doi.org/10.1093/cercor/bhp270>.
- St-Laurent, M., Abdi, H., Burianová, H., Grady, C.L., 2011. Influence of aging on the

- neural correlates of autobiographical, episodic, and semantic memory retrieval. *J. Cogn. Neurosci.* 23 (12), 4150–4163. http://dx.doi.org/10.1162/jocn_a_00079.
- Tambini, A., Ketz, N., Davachi, L., 2010. Enhanced brain correlations during rest are related to memory for recent experiences. *Neuron* 65, 280–290. <http://dx.doi.org/10.1016/j.neuron.2010.01.001>.
- Tzourio-Mazoyer, N., Landeau, B., Papathanassiou, D., Crivello, F., Etard, O., Delcroix, N., Joliot, M., 2002. Automated anatomical labeling of activations in SPM using a macroscopic anatomical parcellation of the MNI MRI single-subject brain. *NeuroImage* 15 (1), 273–289. <http://dx.doi.org/10.1006/nimg.2001.0978>.
- Uddin, L.Q., Supekar, K., Amin, H., Rykhlevskaia, E., Nguyen, D.A., Greicius, M.D., Menon, V., 2010. Dissociable connectivity within human angular gyrus and intraparietal sulcus: evidence from functional and structural connectivity. *Cereb. Cortex* 20 (11), 2636–2646. <http://dx.doi.org/10.1093/cercor/bhq011>.
- Vilberg, K.L., Rugg, M.D., 2007. Dissociation of the neural correlates of recognition memory according to familiarity, recollection, and amount of recollected information. *Neuropsychologia* 45 (10), 2216–2225. <http://dx.doi.org/10.1016/j.neuropsychologia.2007.02.027>.
- Vilberg, K.L., Rugg, M.D., 2008. Memory retrieval and the parietal cortex: a review of evidence from a dual-process perspective. *Neuropsychologia* 46 (7), 1787–1799. <http://dx.doi.org/10.1016/j.neuropsychologia.2008.01.004>.
- Vincent, J.L., Snyder, A.Z., Fox, M.D., Shannon, B.J., Andrews, J.R., Raichle, M.E., Buckner, R.L., 2006. Coherent spontaneous activity identifies a hippocampal-parietal memory network. *J. Neurophysiol.* 96 (6), 3517–3531. <http://dx.doi.org/10.1152/jn.00048.2006>.
- Wagner, A.D., Shannon, B.J., Kahn, I., Buckner, R.L., 2005. Parietal lobe contributions to episodic memory retrieval. *Trends Cogn. Sci.* 9 (9), 445–453. <http://dx.doi.org/10.1016/j.tics.2005.07.001>.
- Wheeler, M., Buckner, R., 2003. Functional dissociation among components of remembering: control, perceived oldness, and content. *J. Neurosci.* 23 (9), 3869–3880. <http://www.jneurosci.org/content/23/9/3869.short>.
- White, T.P., Engen, N.H., Sørensen, S., Overgaard, M., Shergill, S.S., 2014. Uncertainty and confidence from the triple-network perspective: voxel-based meta-analyses. *Brain Cogn.* 85C, 191–200. <http://dx.doi.org/10.1016/j.bandc.2013.12.002>.
- Whitfield-Gabrieli, S., Nieto-Castanon, A., 2012. Conn: a functional connectivity toolbox for correlated and anticorrelated brain networks. *Brain Connect.* 2 (3), 125–141. <http://dx.doi.org/10.1089/brain.2012.0073>.
- Yarkoni, T., Poldrack, R.A., Nichols, T.E., Van Essen, D.C., Wager, T.D., 2011. Large-scale automated synthesis of human functional neuroimaging data. *Nat. Methods* 8 (8), 665–670. <http://dx.doi.org/10.1038/nmeth.1635>.
- Yazar, Y., Bergström, Z.M., Simons, J.S., 2014. Continuous theta burst stimulation of angular gyrus reduces subjective recollection. *PLoS One* 9 (10), e110414. <http://dx.doi.org/10.1371/journal.pone.0110414>.
- Yonelinas, A.P., 2001. Consciousness, control and confidence: the three Cs of recognition memory. *J. Exp. Psychol – Gen.* 130 (3), 361–379.